Tri- and Tetranuclear Mixed-Metal Clusters Containing Alkyne Ligands: Synthesis and Structure of $[Ru_3Ir(CO)_{11}(RCCR')]^-$, $[Ru_2Ir(CO)_9(RCCR')]^-$, and $[HRu_2Ir(CO)_9(RCCR')]$

Vincent Ferrand,[a] Georg Süss-Fink,*[a] Antonia Neels,[a] and Helen Stoeckli-Evans[a]

Keywords: Cluster compounds / Ruthenium / Iridium / Alkynes / Butterfly structures

The tetrahedral cluster anion $[Ru_3Ir(CO)_{13}]^-$ (**1**) reacts with internal alkynes RC≡CR′ to afford the alkyne derivatives $[Ru_3Ir(CO)_{11}(RCCR')]^-$ (**2**: R = R′ = Ph; **3**: R = R′ = Et; **4**: R = Ph; R′ = Me; **5**: R = R′ = Me) which have a butterfly arrangement of the Ru_3Ir skeleton in which the alkyne is coordinated in a μ_4-η^2 fashion. Under CO pressure they undergo fragmentation to give the trinuclear cluster anions $[Ru_2Ir(CO)_9(RCCR')]^-$ (**6**: R = R′ = Ph; **7**: R = R′ = Et; **8**: R = Ph; R′ = Me; **9**: R = R′ = Me), in which the alkyne ligand is coordinated in a μ_3-η^2 parallel fashion. Protonation of these trinuclear anions leads to the formation of the corresponding neutral hydrido clusters $[HRu_2Ir(CO)_9(RC{\equiv}CR')]$ (**10**: R = R′ = Ph; **11**: R = R′ = Et; **12**: R = Ph; R′ = Me; **13**: R = R′ = Me). The protonation of the butterfly anions **2** and **3**, however, gives rise to the formation of the neutral tetrahedral clusters $[HRu_3Ir(CO)_{11}(RCCR')]$ (**14**: R = R′ = Ph and **15**: R = R′ = Et), respectively. The analogous clusters $[HRu_3Ir(CO)_{11}(PhCCCH_3)]$ (**16**) and $[HRu_3Ir(CO)_{11}(CH_3CCCH_3)]$ (**17**) are only accessible from the reaction of the neutral cluster $[HRu_3Ir(CO)_{13}]$ with the corresponding alkynes. The complexes **2**, **4**, **5**, **6**, **10**, **12** and **15** are characterised by X-ray structure analysis.

Introduction

The chemistry of mixed-metal clusters of transition metals has been studied in great detail in recent years,[1][2] stimulated by their possible catalytic potential and the combination of different metals in the same complex.[3a,3b] The mixed-metal cluster $Pt_3Ru_6(CO)_{20}(\mu_3\text{-}PhC_2Ph)(\mu_3\text{-}H)(\mu\text{-}H)$ has been shown by R. D. Adams et al. to be an very active catalyst for the hydrogenation of alkynes[3c−3e]. Tetranuclear clusters with the butterfly structure[4][5] have received much attention, due to their intermediary position between tetrahedral and square-planar clusters. They have been also considered as a model for chemisorption of small molecules,[6] and they have been studied as intermediates in homogeneous catalytic processes.[4,7,8] Both, metal atoms and ligands can vary widely in butterfly-type clusters, which determines, on the one hand, the structural properties of the butterfly framework and, on the other hand, the chemistry of the coordinated ligands.[4]

In a recent publication,[8] we have described the reactivity of the neutral tetrahedral cluster $[HRu_3Ir(CO)_{13}]$[9] towards alkynes and its catalytic potential in hydrogenation reactions. We now report the reaction of its precursor, the cluster anion $[Ru_3Ir(CO)_{13}]^-$[9] with internal alkynes, which affords anionic alkyne clusters of the type $[Ru_3Ir(CO)_{11}(RCCR')]^-$, and we also report on the reactivity of the latter anions towards CO and H^+.

[a] Institut de Chimie, Université de Neuchâtel,
Avenue de Bellevaux 51, CH-2000 Neuchâtel, Switzerland
Fax: (internat.) + 41-32/718-2400
E-mail: Georg.Suess-Fink@ch.unine.ch

Results and Discussion

Synthesis of the Cluster Anions $[Ru_3Ir(CO)_{11}(RCCR')]^-$ (2−5)

The thermal reaction of the tetrahedral cluster anion $[Ru_3Ir(CO)_{13}]^-$ (**1**) with the internal alkynes diphenylacetylene, 3-hexyne, 1-phenyl-1-propyne, or 2-butyne yields, at 90 °C in CH_2Cl_2 solution (pressure Schlenk tube), the alkyne derivatives $[Ru_3Ir(CO)_{11}(RCCR')]^-$ (**2**: R = R′ = Ph; **3**: R = R′ = Et; **4**: R = Ph; R′ = Me; **5**: R = R′ = Me) (Scheme 1). These anions can be isolated as the bis(triphenylphosphoranylidene)ammonium salts from a mixture of diethyl ether and hexane (**2**, **4**, and **5**), or from a mixture of ethanol and pentane (**3**). Complexes **2**, **4**, and **5** gave suitable crystals for X-ray structure analysis.

The infrared spectra of all the compounds display the same absorption pattern in the ν_{co} region, indicating the presence of terminal as well as bridging CO ligands (Table 1). The ^{1}H-NMR spectra of **2**−**5** are complicated by the multiplets of the $[N(PPh_3)_2]^+$ cation; for **2** and **4**, the resonances of the phenyl protons of the alkyne ligands overlap with the signals of the cation. In the case of **4** (containing an unsymmetrical alkyne ligand), only one singlet at δ = 2.82 is observed for the methyl group, indicating the presence of only one isomer. In the case of **3** and **5** (containing a symmetrical alkyne ligand), the two alkyl substituents on the alkyne are nonequivalent, suggesting the alkyne ligand to be coordinated in a nonsymmetrical fashion to the Ru_3Ir framework (Table 1). This is confirmed by the X-ray structure analysis of the bis(triphenylphosphoranylidene)ammonium salts of **2**, **4**, and **5**.

 © WILEY-VCH Verlag GmbH, D-69451 Weinheim, 1999 1434−1948/99/0505−0853 $ 17.50+.50/0

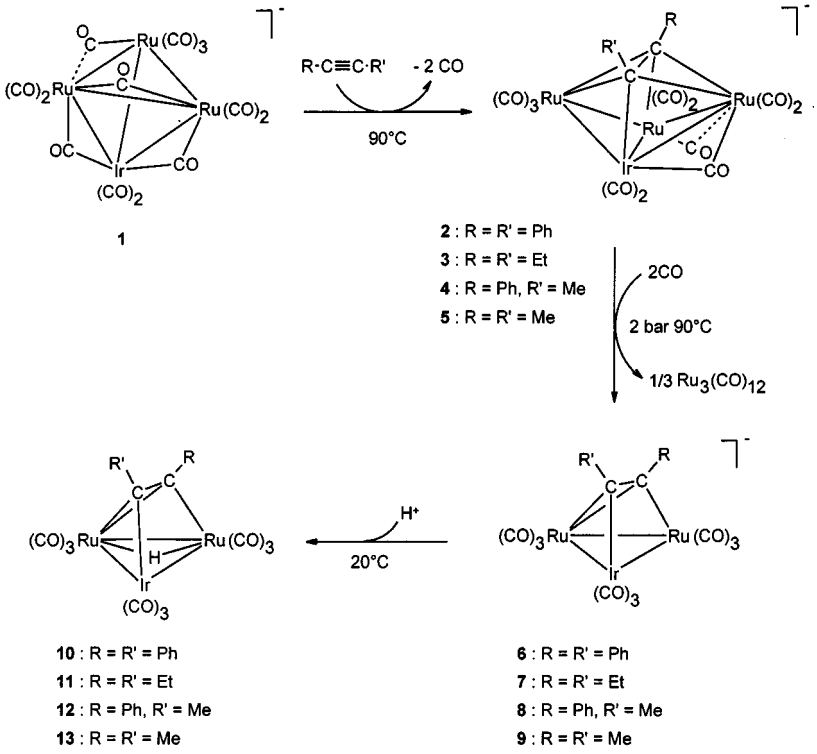

Scheme 1. Synthetic routes to clusters **2**−**13**

Molecular Structures of $[Ru_3Ir(CO)_{11}(RCCR')]^-$ (2, 4, and 5)

Suitable crystals of **2**, **4**, and **5** {$[N(PPh_3)_2]^+$ salts} were grown at room temperature from a mixture of diethyl ether and hexane. The molecular structures of the anions **2**, **4**, and **5** are depicted in Figures 1, 2, and 3, respectively. Selected bond lengths and angles of complexes **2**, **4**, and **5** are summarized in Tables 2, 3, and 4, respectively. The crystal structures consist of discrete $[N(PPh_3)_2]^+$ cations and $[Ru_3Ir(CO)_{11}(RCCR')]^-$ anions showing normal intermolecular contacts between the atoms of the ions. The cluster anions **2**, **4**, and **5** have the same overall structure: The four metal atoms form a butterfly skeleton where the iridium atom occupies a hinge position, whereas in the known cobalt analogue $[Ru_3Co(CO)_{11}(PhCCPh)]^-$,[10] obtained by reaction of $[Ru_3Co(CO)_{13}]^-$ with diphenylacetylene, the cobalt atom occupies a wingtip position. In other mixed-metal clusters anions with the butterfly core structure, such as $[Ru_3M(CO)_{10}Cp(CH_3CCCH_3)]^-$ (M = W, Mo)[11] and $[Co_3Ru(CO)_{10}(PhCCPh)]^-$,[12a] the single metal atom M always occupies a hinge position as found in **2**, **4**, and **5**.

All metal−metal distances in **2**, **4**, and **5** are different (Tables 2, 3, 4), but in the expected range for Ru−Ru and Ru−Ir single bonds.[4,8,9] In the three clusters, the coordination of the eleven carbonyl ligands is the same: While nine carbonyl groups are terminal, one CO ligand [C(6)O(6) in **2**, C(20)O(20) in **4**, C(10)O(10) in **5**] is bridging the Ir−Ru(3) edge, one CO ligand [C(10)O(10) in **2**, C(14)O(14) in **4**, C(15)O(15) in **5**] being coordinated to Ru(2) is semi-

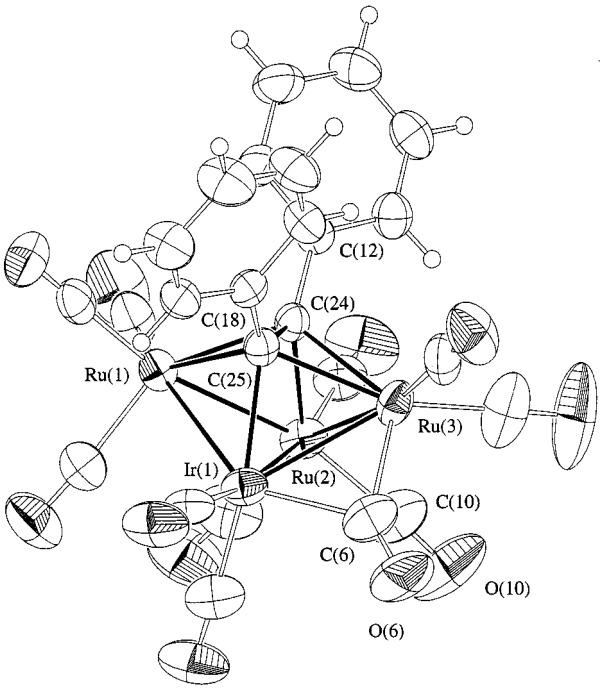

Figure 1. ORTEP plot of $[IrRu_3(CO)_{11}(\mu_4\text{-}\eta^2\text{-}C_2Ph_2)]^-$ (anion **2**); thermal ellipsoids are drawn at 50% of propability

bridging to Ru(3) as indicated by the distances carbon−Ru(2) [**2**: C(10)−Ru(2) = 1.903(7) Å; **4**: C(14)−Ru(2) = 1.896(3) Å; **5**: C(15)−Ru(2) = 1.903(6) Å] and the carbon−Ru(3) [**2**: C(10)−Ru(3) = 2.8893(3) Å; **4**:

Table 1. IR and NMR data of the complexes **2**−**17**

Complexes	ν_{CO} [cm^{-1}][a]	δ (^1H) [ppm][b−d]
$[N(PPh_3)_2][Ru_3Ir(CO)_{11}(PhCCPh)]$ (**2**)	2055(m), 2009(vs), 1988(s), 1960(sh), 1913(w), 1801(w)	7.70−6.80 (C_6H_5, m)
$[N(PPh_3)_2][Ru_3Ir(CO)_{11}(EtCCEt)]$ (**3**)	2052(m), 2002(vs), 1983(s), 1962(sh), 1937(m), 1913(w), 1794(w)	7.70−7.40 (C_6H_5, m); 2.68 ($CH_3CH_2CCCH_2CH_3$, q $^3J_{HH}$ 7.4 Hz); 2.61 ($CH_3CH_2CCCH_2CH_3$, q $^3J_{HH}$ 7.4 Hz); 0.94 ($CH_3CH_2CCCH_2CH_3$, t $^3J_{HH}$ 7.4 Hz); 0.90 ($CH_3CH_2CCCH_2CH_3$, t $^3J_{HH}$ 7.4 Hz)
$[N(PPh_3)_2][Ru_3Ir(CO)_{11}(PhCCMe)]$ (**4**)	2055(m), 2007(vs), 1986(s), 1963(sh), 1936(m), 1909(w), 1799(w)	7.70−7.39 (C_6H_5, m); 2.82 (CH_3CCPh, s)
$[N(PPh_3)_2][Ru_3Ir(CO)_{11}(MeCCMe)]$ (**5**)	2054(m), 2004(vs), 1984(s), 1959(sh), 1934(m), 1906(w), 1800(w)	7.70−7.42 (C_6H_5, m); 3.14 (CH_3CCCH_3, s); 2.91 (CH_3CCCH_3, s)
$[N(PPh_3)_2][Ru_2Ir(CO)_9(PhCCPh)]$ (**6**)	2054(m), 2011(s), 1998(vs), 1980(s), 1940(m)	6.60−7.70 (C_6H_5, m)
$[N(PPh_3)_2][Ru_2Ir(CO)_9(EtCCEt)]$ (**7**)	2048(w), 2002(s), 1992(vs), 1971(m), 1932(w)	7.70−7.20 (C_6H_5, m); 3.41 ($CH_{3c}CH_aH_bCCCH_{a'}H_{b'}CH_{3c'}$, dq $^3J_{HaHc}$ 7.2 Hz, $^2J_{HaHb}$ 13.3 Hz); 2.74 ($CH_{3c}CH_aH_bCCCH_{a'}H_{b'}CH_{3c'}$, dq $^3J_{Ha'Hc'}$ 7.3 Hz, $^2J_{Ha'Hb'}$ 13.0 Hz); 2.10 ($CH_{3c}CH_aH_bCCCH_{a'}H_{b'}CH_{3c'}$, dq $^3J_{HbHc}$ 7.2 Hz, $^2J_{HaHb}$ 13.3 Hz); 1.97 ($CH_{3c}CH_aH_bCCCH_{a'}H_{b'}CH_{3c'}$, dq $^3J_{Hb'Hc'}$ 7.3 Hz, $^2J_{Ha'Hb'}$ 13.0 Hz);1.14 ($CH_{3c}CH_aH_bCCCH_{a'}H_{b'}CH_{3c'}$, t $^3J_{HH}$ 7.3 Hz); 1.07 ($CH_{3c}CH_aH_bCCCH_{a'}H_{b'}CH_{3c'}$, t $^3J_{HH}$ 7.3 Hz);
$[N(PPh_3)_2][Ru_2Ir(CO)_9(PhCCMe)]$ (**8**)	2052(w), 2007(s), 1996(vs), 1976(m), 1938(w)	7.70−6.90 (C_6H_5, m); 2.64 (CH_3CCPh, s(isomer 1)); 2.30 (CH_3CCPh, s(isomer 2))
$[N(PPh_3)_2][Ru_2Ir(CO)_9(MeCCMe)]$ (**9**)	2049(w), 2002(s), 1993(vs), 1971(m), 1934(w)	7.71−7.35 (C_6H_5, m); 2.70 (CH_3CCCH_3, s); 2.40 (CH_3CCCH_3, s)
$[HRu_2Ir(CO)_9(PhCCPh)]$ (**10**)	2101(w), 2072(vs), 2061(s), 2034(s), 2022(m), 2016(m), 2005(w)	7.20−6.80 (C_6H_5, m); −15.07 (Ru*H*Ru, s)
$[HRu_2Ir(CO)_9(EtCCEt)]$ (**11**)	2099(w), 2069(s), 2057(s), 2030(vs), 2018(m), 2008(m), 1990(w)	2.93 ($CH_3CH_2CCCH_2CH_3$, q $^3J_{HH}$ 7.4 Hz); 2.42 ($CH_3CH_2CCCH_2$ CH_3, q $^3J_{HH}$ 7.4 Hz); 1.34 ($CH_3CH_2CCCH_2CH_3$, t $^3J_{HH}$ 7.4 Hz); 1.20 ($CH_3CH_2CCCH_2CH_3$, t $^3J_{HH}$ 7.4 Hz); −15.39 (Ru*H*Ru, s)
$[HRu_2Ir(CO)_9(PhCCMe)]$ (**12**)	2100(w), 2071(vs), 2060(s), 2032(s), 2021(m), 2003(m), 1994(w)	7.20−6.90 (C_6H_5, m); 2.80 (CH_3CCPh, s); −15.27 (Ru*H*Ru, s)
$[HRu_2Ir(CO)_9(MeCCMe)]$ (**13**)	2099(w), 2069(vs), 2057(s), 2030(vs), 2018(m), 2008(m), 1991(w)	2.83 (CH_3CCCH_3, s); 2.37 (CH_3CCCH_3, s); −15.31 (Ru*H*Ru, s)
$[HRu_3Ir(CO)_{11}(PhCCPh)]$ (**14**)	2095(w), 2071(s), 2053(s), 2037(vs), 2012(m), 1994(m), 1842(w)	7.30−7.00 (C_6H_5, m); −18.88 (Ru*H*Ru, s)
$[HRu_3Ir(CO)_{11}(EtCCEt)]$ (**15**)	2095(w), 2070(s), 2051(s), 2034(vs), 2010(m), 1991(m), 1840(w)	2.98 ($CH_3CH_aH_bCCCH_{a'}H_{b'}CH_3$, dq $^3J_{HH}$ 7.3 Hz, $^2J_{HH}$ 15.0 Hz); 2.74 ($CH_3CH_aH_bCCCH_{a'}H_{b'}CH_3$, dq $^3J_{HH}$ 7.3 Hz, $^2J_{HH}$ 15.0 Hz); 1.28 ($CH_3CH_aH_bCCCH_{a'}H_{b'}CH_3$, t $^3J_{HH}$ 7.3 Hz); −19.10 (Ru*H*Ru, s)
$[HRu_3Ir(CO)_{11}(PhCCMe)]$ (**16**)	2093(w), 2065(s), 2048(s), 2032(vs), 2006(m), 1989(m), 1842(w)	7.50−7.20 (C_6H_5, m); 2.80 (CH_3, s) −18.88 (Ru*H*Ru, s)
$[HRu_3Ir(CO)_{11}(MeCCMe)]$ (**17**)	2094(w), 2068(s), 2049(s), 2033(vs), 2009(m), 1988(m), 1844(w)	2.72 (CH_3, s); −18.98 (Ru*H*Ru, s)

[a] Recorded in ether (**2**−**5**), CH_2Cl_2 (**6**−**9**, **14**−**17**), hexane (**10**−**12**, **13**). − [b] Measured in $CDCl_3$ solution at 294 K at 200 MHz (**2**, **4**−**6**, **9**, **10**, **12**−**15**, **17**). − [c] Measured in $CDCl_3$ solution at 294 K at 400 MHz (**3**, **7**, **8**, **11**, **16**). − [d] Measured in $CDCl_3$ solution at 215 K at 400 MHz (**7**, **8**).

C(14)−Ru(3) = 2.8115(3) Å; **5**: C(15)−Ru(3) = 2.8613(7) Å]. The angles C(10)−Ru(2)−Ru(3) = 73.7(2)° (**2**), C(14)−Ru(2)−Ru(3) = 71.86(10)° (**4**), C(15)−Ru(2)−Ru(3) = 73.00(19)° (**5**) are found to be similar to the angle observed in the cluster anion $[FeRu_3(CO)_{12}NO]^-$ [13] for a semibridging CO group.[14] These findings are comfirmed by the infrared spectra of **2**−**5** which exhibit a ν_{co} absorption around 1920 cm^{-1}.

The alkyne ligand in **2**, **4**, and **5** is coordinated to the Ru_3Ir metal core in a μ_4-η^2 fashion. One of the carbon atoms is σ-bonded to Ir, whereas the second one is σ-bonded to Ru(2), both carbon atoms being π-bonded to Ru(1) and Ru(3). This observation is confirmed by the ^1H-NMR spectra of **3** and **5** which display two different chemical shifts for the two ethyl or methyl substituents, respectively. The carbon−carbon bond is closer to Ru(1) than to Ru(3) in the three clusters, the torsion angle between the carbon−carbon backbone and the Ir(1)−Ru(2) edge is close to 0° [**2**: 0.0°(18); **4**: −0.04(11); **5**: 0.3°(2)] indicating that these two bonds are almost parallel.

With an electron count of 60e, **2**, **4**, and **5** are electron-deficient, since an M_4 butterfly cluster consistent with the noble-gas rule would require 62 electrons. However, considering **2**, **4**, and **5** as octahedral Ru_3IrC_2 clusters, an electron count of 60e is consistent with Wade's rules which predict a *closo* structure.[15]

Synthesis of $[Ru_2Ir(CO)_9(RCCR')]^-$ (6−9)

The cluster anions $[Ru_3Ir(CO)_{11}(RCCR')]^-$ (**2**: R = R′ = Ph; **3**: R = R′ = Et; **4**: R = Ph; R′ = Me; **5**: R = R′ = Me) undergo fragmentation of the metal core under CO pressure (2 bar) at 90 °C to give the trinuclear alkyne cluster anions $[Ru_2Ir(CO)_{11}(RCCR')]^-$ (Scheme 1). They can be isolated as the bis(triphenylphosphoranylidene)ammonium salts from a mixture of CH_2Cl_2 and diethyl ether (**6**) or from ethanol and pentane (**7**−**9**). The loss of metal fragments from a cluster has already been observed;[16][17] for example the cluster anion $[RuCo_3(CO)_{10}(\mu_4\text{-}\eta^2\text{-}C_2Ph_2)]^-$ can release a "Co(CO)" fragment to give the trinuclear complex $[RuCo_2(CO)_9(\mu_3\text{-}\eta^2\text{-}C_2Ph_2)]$ in which the alkyne adopts a parallel coordination.[12][18]

The infrared spectra of **6**−**9** exhibit in the carbonyl region absorptions of only terminal CO ligands (Table 1). The room-temperature ^1H-NMR spectrum of **8** reveals, in addition to the signals of the $[N(PPh_3)_2]^+$ cation, two singlets for the methyl group of the MeCCPh ligand in a ratio of

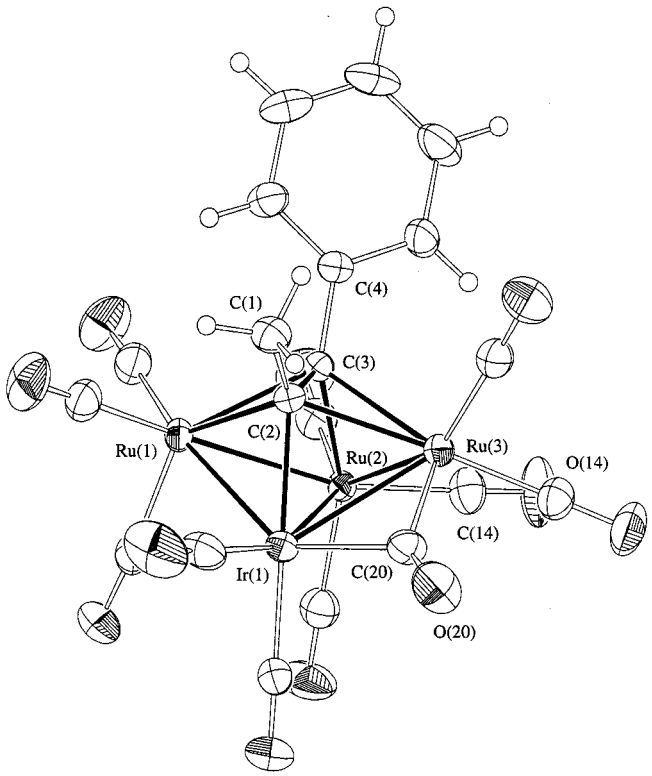

Figure 2. ORTEP plot of $[IrRu_3(CO)_{11}(\mu_4\text{-}\eta^2\text{-}PhCCMe)]^-$ (anion **4**); thermal ellipsoids are drawn at 50% of propability

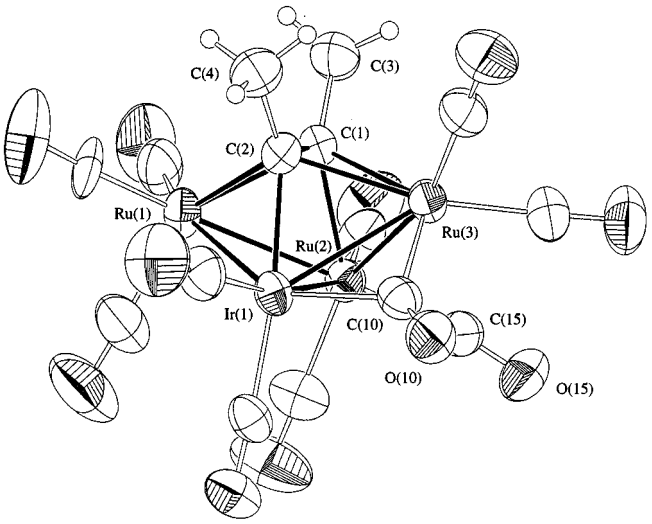

Figure 3. ORTEP plot of $[IrRu_3(CO)_{11}(\mu_4\text{-}\eta^2\text{-}C_2Me_2)]^-$ (anion **5**); thermal ellipsoids are drawn at 50% of propability

45:55. This ratio does not change down to −58 °C ($CDCl_3$), suggesting the presence of two isomers.[19−22] In the case of $[Ru_2Ir(CO)_9(MeCCMe)]^-$ (**9**), two singlets for the methyl substituents are observed in a ratio of 1:1, because the chemical environment of each CCH_3 moiety is different. The spectrum of $[Ru_2Ir(CO)_9(EtCCEt)]^-$ (**7**) is more complicated, presenting a temperature dependence of the signals of the ethyl substituents: At room temperature, four broad signals for the hydrogen atoms of the methylene groups are observed, resulting in four well-resolved multiplets at −58 °C, in a ratio of 1:1:1:1. In a selective decoupling experiment by irradiating at the resonances of the methyl proton, the four methylene multiplets resolve into four doublets with a coupling constant of 13 Hz, showing the protons of each methylene group to be diastereotopic (Table 1).[20,22a,22c,23a]

Table 2. Selected bond lengths [Å], bond angles [°], and torsion angles [°] for the anion **2**; estimated standard deviations in parentheses

Ir(1)−Ru(1)	2.7223(5)	Ru(3)−C(25)	2.298(4)
Ir(1)−Ru(3)	2.7235(6)	Ru(3)−C(24)	2.335(4)
Ir(1)−Ru(2)	2.7756(5)	Ru(3)−C(6)	1.993(6)
Ir(1)−C(6)	2.133(7)	C(24)−C(25)−C(18)	126.1(4)
Ir(1)−C(25)	2.188(4)	C(25)−C(24)−C(12)	127.1(4)
Ru(1)−Ru(2)	2.7357(6)	O(6)−C(6)−Ir(1)	134.9(6)
Ru(1)−C(25)	2.242(4)	O(6)−C(6)−Ru(3)	142.5(6)
Ru(1)−C(24)	2.258(5)	C(10)−Ru(2)−Ru(3)	73.7(2)
C(24)−C(25)	1.443(6)	O(10)−C(10)−Ru(2)	173.6(7)
		C(25)−Ir(1)−-Ru(2)−C(24)	0.00(18)

Table 3. Selected bond lengths [Å], bond angles [°], and torsion angles [°] for the anion **4**; estimated standard deviations in parentheses

Ir(1)−Ru(1)	2.7025(4)	Ru(3)−C(2)	2.338(3)
Ir(1)−Ru(3)	2.7018(4)	Ru(3)−C(3)	2.375(3)
Ir(1)−Ru(2)	2.8690(4)	Ru(3)−C(20)	1.977(3)
Ir(1)−C(20)	2.105(3)	C(1)−C(2)−C(3)	124.8(2)
Ir(1)−C(2)	2.132(3)	C(2)−C(3)−C(4)	123.5(2)
Ru(1)−Ru(2)	2.7158(5)	O(20)−C(20)−Ir(1)	135.5(3)
Ru(1)−C(2)	2.282(3)	O(20)−C(20)−Ru(3)	141.6(3)
Ru(1)−C(3)	2.297(3)	C(14)−Ru(2)−Ru(3)	71.86(10)
Ru(2)−Ru(3)	2.7483(5)	O(14)−C(14)−Ru(2)	167.4(3)
Ru(2)−C(14)	1.896(3)	C(3)−Ru(2)−Ir(1)−C(2)	0.04(11)
Ru(2)−C(3)	2.151(3)	C(2)−C(3)	1.429(4)

Table 4. Selected bond lengths [Å], bond angles [°], and torsion angles [°] for the anion **5**; estimated standard deviations in parentheses

Ir(1)−Ru(1)	2.7044(7)	Ru(3)−C(1)	2.356(6)
Ir(1)−Ru(3)	2.7182(7)	Ru(3)−C(2)	2.321(5)
Ir(1)−Ru(2)	2.8000(8)	Ru(3)−C(10)	2.012(6)
Ir(1)−C(10)	2.125(6)	C(3)−C(1)−C(2)	123.7(5)
Ir(1)−C(2)	2.150(6)	C(1)−C(2)−C(4)	124.3(5)
Ru(1)−Ru(2)	2.7114(9)	O(10)−C(10)−Ir(1)	136.1(5)
Ru(1)−C(1)	2.272(5)	O(10)−C(10)−Ru(3)	141.8(5)
Ru(1)−C(2)	2.242(6)	C(15)−Ru(2)−Ru(3)	73.00(19)
Ru(2)−Ru(3)	2.7647(8)	O(15)−C(15)−Ru(2)	170.5(6)
Ru(2)−C(1)	2.154(6)	C(2)−Ir(1)−Ru(2)−C(1)	0.3(2)
Ru(2)−C(15)	1.903(6)	C(1)−C(2)	1.406(8)

Molecular Structure of $[Ru_2Ir(CO)_9(PhCCPh)]^-$(6)

The molecular structure of **6** was confirmed by a single-crystal X-ray structure analysis of the bis(triphenylphosphoranylidene)ammonium salt. Suitable crystals were obtained by slow diffusion of diethyl ether into a concentrated dichloromethane solution at room temperature. The molecular structure of the anion is depicted in Figure 4. Selected bond lengths and angles are presented in Table 5. The crystal structure consists of discrete $[N(PPh_3)_2]^+$ cations and

$[Ru_2Ir(CO)_9(PhCCPh)]^-$ anions showing normal intermolecular contacts between the atoms of the ions. The ruthenium and iridium atoms of the cluster anion form a closed triangle in which all the metal−metal distances are different but within the range of Ru−Ru and Ir−Ru single bonds (Table 5). Each metal atom is bonded to three terminal CO groups.

Table 5. Selected bond lengths [Å], bond angles [°], and torsion angles [°] for the anion **6**; estimated standard deviations in parentheses

Ir(1)−Ru(1)	2.7120(8)	Ru(2)−C(1)	2.096(8)
Ir(1)−Ru(2)	2.7952(10)	Ru(2)−C(1)	2.096(8)
Ir(1)−C(2)	2.117(8)	C(1)−C(2)	1.363(11)
Ru(1)−Ru(2)	2.7084(11)	C(1)−C(2)−C(3)	125.4(7)
Ru(1)−C(1)	2.260(8)	C(2)−C(1)−C(9)	123.5(7)
Ru(1)−C(2)	2.246(8)	C(9)−C(1)−C(2)−C(3)	−9.8(13)

The alkyne ligand is coordinated in a classical μ_3-η^2 fashion over the metal triangle[18] as observed in $[Co_2Ru(CO)_9(C_2Ph_2)]$[12] The C(1)−C(2) backbone is almost parallel to the Ir(1)−Ru(2) edge [C(2)−Ir(1)−Ru(2)−C(1) 1.2(3)°]. The carbon atoms C(1) and C(2) are σ-coordinated to Ir(1) and Ru(2), respectively, and are both π-bonded to Ru(1).

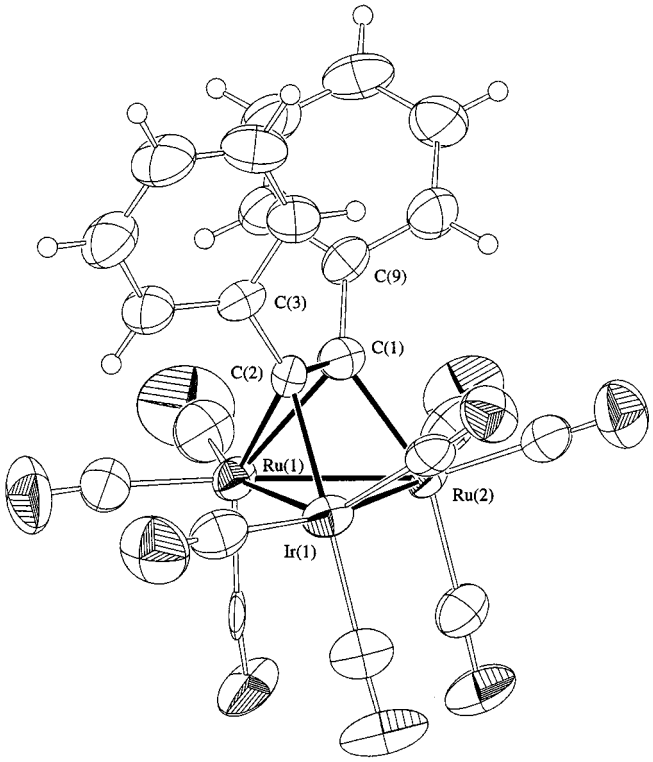

Figure 4. ORTEP plot of $[IrRu_2(CO)_9(\mu_3\text{-}\eta^2\text{-}C_2Ph_2)]^-$ (anion **6**); thermal ellipsoids are drawn at 50% of propability

The carbon−carbon bond is shorter in **6** [C(1)−C(2) 1.363(11) Å] than in **2** [C(24)−C(25) 1.443(6) Å]. This is due to the coordination of the alkyne to only three metal atoms in **6** with respect to **2** where it is coordinated to four metal atoms. The carbon−carbon bond length in **6** [C(1)−C(2) 1.363(11) Å] compares well with that in $[Co_2Ru(CO)_9(C_2Ph_2)]$ (C−C 1.370(3) Å)[12] and related complexes in which the C−C bond length varies from 1.33 to 1.47 Å.[18] Clusters **6**−**9** have the expected electron count of 48e for trinuclear clusters which obey the noble gas rule.

Synthesis of $[HRu_2Ir(CO)_9(RCCR')]$ (10−13)

The reaction of the anions $[Ru_2Ir(CO)_9(RCCR')]^-$ (**6**−**9**) with an excess of $HBF_4 \cdot OEt_2$ at room temperature leads to the formation of the neutral hydrido clusters $[HRu_2Ir(CO)_9(RCCR')]$ (**10**: R = R′ = Ph; **11**: R = R′ = Et; **12**: R = Ph; R′ = Me; **13**: R = R′ = Me), which can be isolated by chromatographic methods and recrystallized from hexane at −18 °C (Scheme 1).

The infrared spectra of **10**−**13** display an almost identical ν_{co} absorption pattern in the region of terminal carbonyl ligands (Table 1). The ^{1}H-NMR spectra of **10**−**13** indicate, in addition to the signals of the alkyne substituents, the resonance of a bridging hydrido ligand at around δ = −15 (Table 1). In all cases, only one isomer is observed. For $[HRu_2Ir(CO)_9(EtCCEt)]$ (**11**) and $[HRu_2Ir(CO)_9(MeCCMe)]$ (**13**), the two ethyl or methyl groups are found to be nonequivalent.

Molecular Structure of $[HRu_2Ir(CO)_9(RCCR')]$ (10, 12)

Suitable crystals of $[HRu_2Ir(CO)_9(PhCCPh)]$ (**10**) and $[HRu_2Ir(CO)_9(PhCCMe)]$ (**12**) have been obtained from a concentrated hexane solution at −18 °C. The molecular structure of **10** is depicted in Figure 5 and that of **12** in Figure 6. Selected bond lengths and angles are presented in Tables 6 and 7. The crystal-structure analysis of **10** reveals two independent molecules per asymmetric unit of the unit cell, which have the same constitution, but differ slightly in bond lengths and angles.

The two clusters **10** and **12** have the same overall structure, showing the same carbonyl and alkyne coordination. The three metal atoms form a closed triangle. Each metal atom is bonded to three terminal CO groups. In both complexes the longer Ru(1)−Ru(2) distance [**10**: 2.7965(10); **12**: 2.7943(7) Å] suggests the presence of the hydrido bridge across this edge.

The alkyne ligand is coordinated in a μ_3-η^2 fashion over the Ru_2Ir framework as also found in cluster **6**. All carbon−carbon and carbon−metal distances compare well with those in other $M_3(\mu_3\text{-}\eta^2\text{-}RCCR')$ complexes.[18] The neutral complexes $[HRu_2Ir(CO)_9(RCCR')]$ (**10**−**13**) have, as the anions **6**−**9**, the expected electron count of 48e.

Reaction of $[Ru_3Ir(CO)_{11}(RCCR')]^-$ with $HBF_4 \cdot OEt_2$

Protonation of the anions $[Ru_3Ir(CO)_{11}(RCCR')]^-$ gives different results depending on the nature of the coordinated alkyne ligand. For R = R′ = Ph (**14**) or R = R′ = Et (**15**), the neutral hydrido complexes $[HRu_3Ir(CO)_{11}(PhCCPh)]$

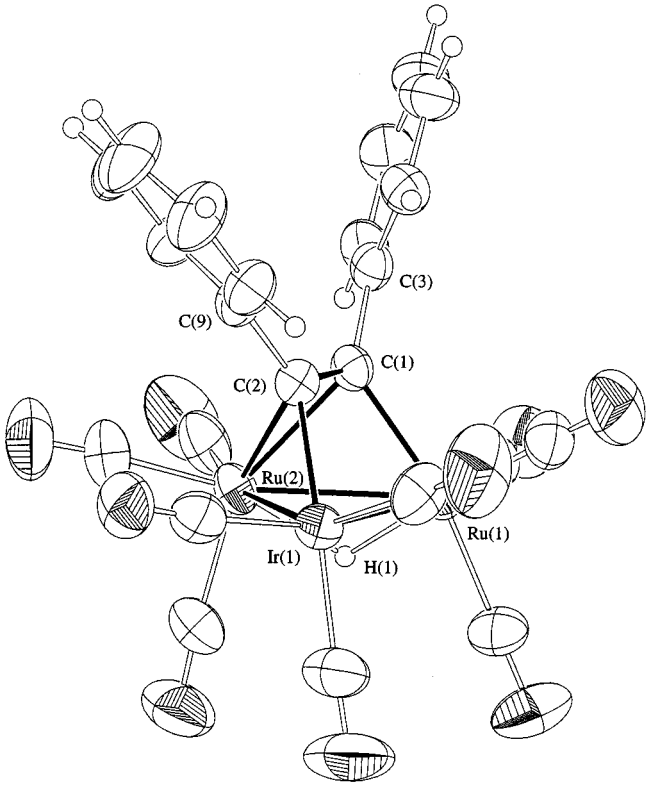

Figure 5. ORTEP plot of $[HIrRu_2(CO)_9(\mu_3\text{-}\eta^2\text{-}C_2Ph_2)]$ **10**; thermal ellipsoids are drawn at 50% of propability

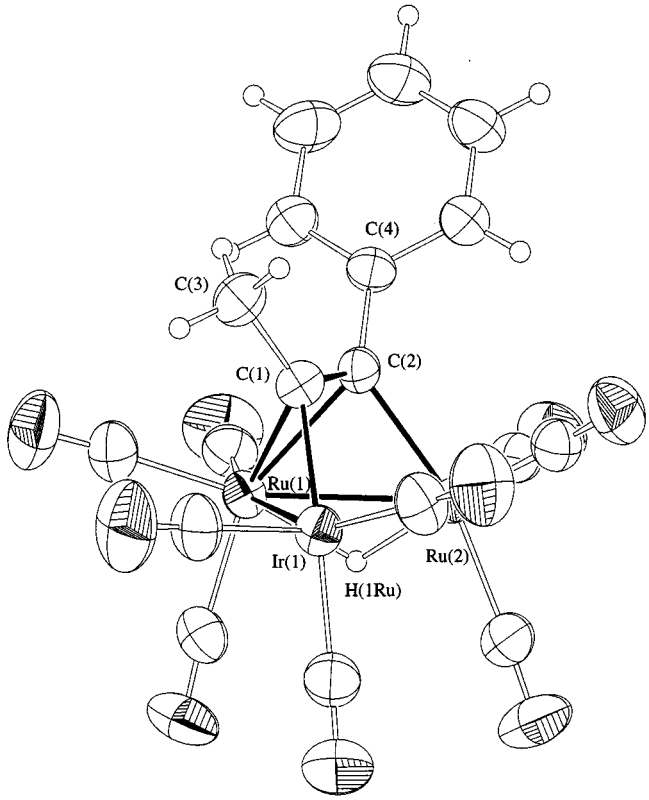

Figure 6. ORTEP plot of $[HIrRu_2(CO)_9(\mu_3\text{-}\eta^2\text{-}PhCCMe)]$ **12**; thermal ellipsoids are drawn at 50% of propability

Table 6. Selected bond lengths [Å], bond angles [°], and torsion angles [°] for **10**; estimated standard deviations in parentheses

Molecule A		Molecule B	
Ir(1)−Ru(2)	2.6901(7)	Ir(2)−Ru(4)	2.6936(9)
Ir(1)−Ru(1)	2.7523(8)	Ir(2)−Ru(3)	2.7517(8)
Ir(1)−C(2)	2.076(6)	Ir(2)−C(25)	2.080(6)
Ru(1)−Ru(2)	2.7965(10)	Ru(3)−C(24)	2.119(7)
Ru(1)−C(1)	2.113(7)	Ru(3)−Ru(4)	2.7938(9)
Ru(1)−H(1)	1.77(11)	Ru(3)−H(2)	1.63(11)
Ru(2)−C(1)	2.295(6)	Ru(4)−C(25)	2.310(6)
Ru(2)−C(2)	2.307(6)	Ru(4)−C(24)	2.325(7)
Ru(2)−H(1)	1.85(11)	Ru(4)−H(2)	1.91(11)
C(1)−C(2)	1.374(9)	C(24)−C(25)	1.375(9)
C(2)−C(1)−C(3)	123.9(6)	C(25)−C(24)−C(26)	124.4(6)
C(1)−C(2)−C(9)	125.0(6)	C(24)−C(25)−C(32)	124.9(6)
C(3)−C(1)−C(2)−C(9)	8.7(10)	C(26)−C(24)−C(25)−C(32)	−6.5(10)

Table 7. Selected bond lengths [Å], bond angles [°], and torsion angles [°] for **12**; estimated standard deviations in parentheses

Ir(1)−Ru(1)	2.6924(6)	Ru(2)−C(2)	2.111(6)
Ir(1)−Ru(2)	2.7578(5)	Ru(2)−H(1Ru)	1.78(7)
Ir(1)−C(1)	2.074(6)	C(1)−C(2)	1.372(9)
Ru(1)−Ru(2)	2.7943(7)	C(2)−C(1)−C(3)	123.9(6)
Ru(1)−C(2)	2.285(6)	C(1)−C(2)−C(4)	124.4(5)
Ru(1)−C(1)	2.318(6)	C(3)−C(1)−C(2)−C(4)	−0.3(10)
Ru(1)−H(1Ru)	1.81(7)		

(**14**) and $[HRu_3Ir(CO)_{11}(EtCCEt)]$ (**15**) are formed (Scheme 2). When R or R′ is a methyl group, the reaction does not afford the neutral hydrido complex, but leads to an unidentified green decomposition product. The expected clusters $[HRu_3Ir(CO)_{11}(PhCCMe)]$ (**16**) and $[HRu_3Ir(CO)_{11}$-(MeCCMe)] (**17**) are, however, accessible from the reaction of the neutral hydrido cluster $[HRu_3Ir(CO)_{13}]$ with the corresponding alkyne (Scheme 2). Clusters **14** and **17** have already been reported[8] and they are included here for the sake of completeness.

The infrared spectra of **14**−**17** display in the ν_{co} region the same absorption pattern: Five bands are assigned to terminal CO ligands and one absorption around 1840 cm^{-1} corresponds to a bridging CO group (Table 1). In the ^{1}H-NMR spectra of **14**−**17**, the hydrido ligand resonates as a singlet around $\delta = -19$. In **15** the ethyl substituents of the alkyne ligand are found to be equivalent, but the two hydrogen atoms of the methylene groups are diastereotopic (Table 1). The molecular structure of **15** is confirmed by a single-crystal X-ray structure analysis.

Molecular Structure of $[HRu_3Ir(CO)_{11}(EtCCEt)]$ (15)

Suitable crystals of **15** were grown at −18 °C in hexane. The molecular structure of **15** is depicted in Figure 7. Selected bond lengths and angles of **15** are listed in Table 8. The complex **15** has the same overall structure as found in **14** and **17**,[8] showing the same carbonyl, alkyne and hydride coordination pattern.

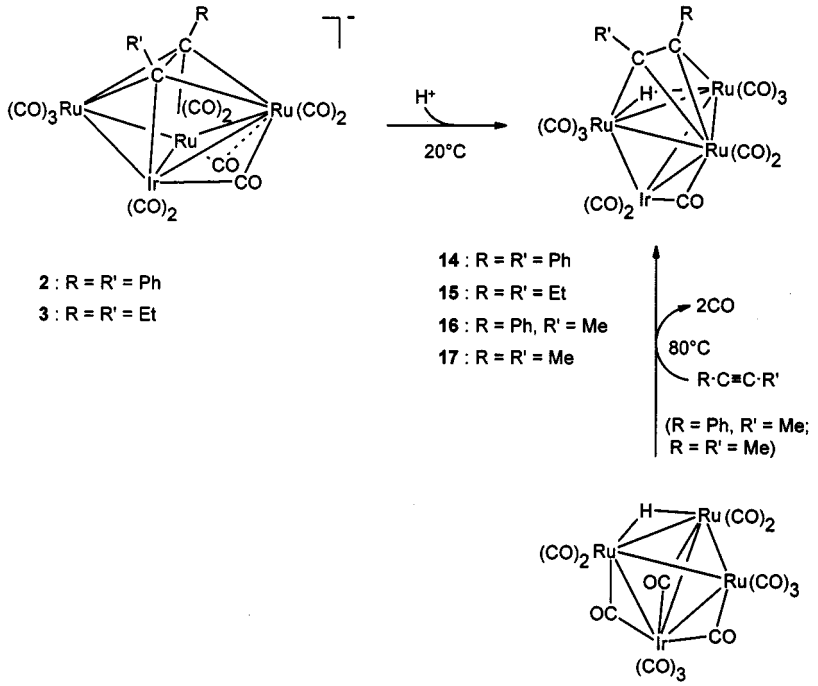

Scheme 2. Synthetic routes to clusters **14**−**17**

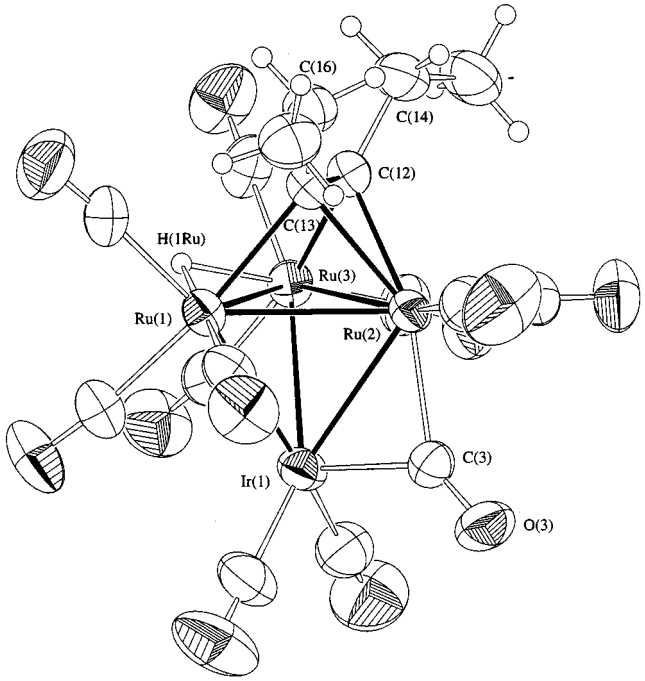

Figure 7. ORTEP plot of $[HIrRu_3(CO)_{11}(\mu_3\text{-}\eta^2\text{-}C_2Et_2)]$ **15**; thermal ellipsoids are drawn at 50% of propability

The four metal atoms form a tetrahedron in which the Ru−Ir distances vary from 2.7228(11) to 2.7833(8) Å and the Ru−Ru distances from 2.7981(10) to 2.8514(9) Å, in accordance with metal−metal single bonds.[8] The cluster **15** presents, as expected for a tetrahedral arrangement, an electron count of 60 e. The short distance Ru(2)−Ir [2.7228(11) Å] is due to the bridging carbonyl ligand over this edge. The base of the tetrahedron is composed of three ruthenium atoms. The longer Ru(1)−Ru(3) distance [2.8514(9) Å] suggests the presence of the hydrido bridge across this edge. Two of the three ruthenium atoms are bonded to three terminal CO groups, whereas Ru(2) and Ir are bonded to two terminal CO groups and share the bridging CO ligand. The alkyne is coordinated in a μ_3-η^2-bonding mode over the Ru_3 face of the tetrahedron. Due to the coordination of the alkyne group to the metal core, the carbon−carbon bond is lengthened [C(12)−C(13) 1.395(11) Å], but is in the range observed in **14**, **17**,[8] and other clusters such as $HCpWOs_3[\mu_3\text{-}\eta^2\text{-}C_2(Tol)_2]$.[24][25]

Table 8. Selected bond lengths [Å], bond angles [°], and torsion angles [°] for **15**; estimated standard deviations in parentheses

Ir(1)−Ru(1)	2.7727(9)	Ru(2)−C(12)	2.183(7)
Ir(1)−Ru(2)	2.7228(11)	Ru(2)−C(13)	2.168(7)
Ir(1)−Ru(3)	2.7833(8)	Ru(3)−C(12)	2.149(8)
Ru(1)−Ru(2)	2.7981(10)	Ru(3)−H(1Ru)	1.75(6)
Ru(1)−Ru(3)	2.8514(9)	C(12)−C(13)	1.395(11)
Ru(1)−C(13)	2.154(7)	C(13)−C(12)−C(14)	121.7(7)
Ru(1)−H(1Ru)	1.81(6)	C(12)−C(13)−C(16)	122.7(7)
Ru(2)−Ru(3)	2.8110(9)	C(14)−C(12)−C(13)−C(16)	0.4(11)

Conclusions

The Ru_3Ir framework shows a great fexibility with respect to the coordination of alkyne ligands: The tetrahedral metal skeleton in $[Ru_3Ir(CO)_{13}]^-$ (**1**) opens up upon coordination of an alkyne ligand to give a butterfly framework in $[Ru_3Ir(CO)_{11}(RCCR)]^-$ (**2**−**5**). Protonation of the butterfly clusters **2** and **3** leads, with closure of the Ru−Ru bond, back to a tetrahedral metal skeleton in the neutral clusters $[HRu_3Ir(CO)_{11}(RCCR')]$ (**14**−**15**). The second important

feature is the fragmentation of the tetranuclear anions in $[Ru_3Ir(CO)_{11}(RCCR)]^-$ (**2**−**5**) under CO pressure to give the trinuclear anions $[Ru_2Ir(CO)_9(RCCR)]^-$ (**6**−**9**). In a comparison of the 3-hexyne complexes, it is interesting to note that in the case of **3** and **11**, the two protons of the two different CH_2 groups of the 3-hexyne ligand are equivalent, whereas in **7** and **15** they are nonequivalent (diastereotopic). In the case of the tetranuclear cluster $[Ru_3Ir(CO)_{11}(EtCCEt)]^-$ (**3**) the averaging of the methylene protons may be explained by a carbonyl fluxionality involving the bridging and semi-bridging carbonyl ligands which could brigde equally well to both wingtip ruthenium atoms. In the case of the trinuclear cluster $[HRu_2Ir(CO)_9(EtCCEt)]$ (**11**), the μ_3-alkyne ligand itself might be fluxional on the trinuclear metal core, as observed in $[H_2Ru_3(CO)_9(EtCCEt)]$,[22a] $[Co_2Ru(CO)_9(EtCCEt)]$,[19] $[FeCo_2(CO)_9(EtCCEt)]$,[21] $[CpNiCoM(CO)_6(EtCCEt)]$ (M = Fe, Ru, Os),[23a] $[H_2Os_3(CO)_9(C_9H_6)]$.[23b]

Experimental Section

General: All reactions were carried out under pure nitrogen with standard Schlenk techniques. Solvents were destilled with appropriate drying agents, deoxygenated, and nitrogen-saturated prior to use.[26] − Preparative thin-layer chromatography was performed using 20 cm × 20 cm plates coated with Fluka silica gel G. The starting complexes $[Ru_3Ir(CO)_{13}]^-$ and $[HRu_3Ir(CO)_{13}]$ were prepared according to a published method.[9] − Diphenylacetylene was purchased from Fluka; 3-hexyne, 1-phenyl-1-propyne, and 2-butyne were purchased from Aldrich and used as recieved. − NMR spectra were recorded with a Varian Gemini 200 BB or a Bruker AMX 400 spectrometer, using the resonance of the residual protons of the deuterated solvents as reference. − Infrared spectra were recorded with a Perkin−Elmer 1720X FT IR spectrometer. − Micro-analyses were carried out by the Mikroelementaranalytisches Laboratorium of the ETH Zürich, Switzerland.

Preparations

$[N(PPh_3)_2][Ru_3Ir(CO)_{11}(RCCR')]$ (Anions 2−5): A solution of $[N(PPh_3)_2][Ru_3Ir(CO)_{13}]$ (anion **1**) (100 mg, $7.15\bullet10^{-2}$ mmol) in CH_2Cl_2 (30 mL) was stirred with an excess of RC≡CR′ (**2**: 38 mg, $21.46\bullet10^{-2}$ mmol; **3**: 24 μL, $21.46\bullet10^{-2}$ mmol; **4**: 27 μL, $21.46\bullet10^{-2}$ mmol; **5**: 17 μL, $21.46\bullet10^{-2}$ mmol) at 90 °C in a pressure Schlenk tube. During the reaction the pressure was released once. The reaction was followed by infrared spectroscopy; after 2.5 h, the IR spectrum in the ν_{CO} region indicated the complete desappearance of the starting complex **1**. Then the solvent was evaporated and the red-orange oil was washed three times with 10 mL of hexane to remove the excess of the unreacted alkyne. The residue was dissolved in 20 mL of Et_2O, and the solution was filtered. Dark-red air-stable crystals of the $[N(PPh_3)_2]^+$ salts of **2**, **4**, **5** were obtained by slow evaporation (room temperature) of a diethyl ether/hexane solution. The crystals were dried in vacuo. − **2**: Yield 92 mg (85%). − $C_{61}H_{40}IrNO_{11}P_2Ru_3$ (1520.36): calcd. C 48.19, H 2.65, N 0.92; found C 48.32, H 2.58, N 0.93. − **4**: Yield 83 mg (80%). − $C_{56}H_{38}O_{11}NP_2Ru_3Ir$ (1458.28): calcd. C 46.12, H 2.63, N 0.96, found C 45.94, H 2.37, N 1.00. − **5**: Yield 75 mg (75%). − $C_{51}H_{36}O_{11}NP_2Ru_3Ir$ (1396.22): calcd. C 43.87, H 2.60, N 1.00; found C 43.77, H 2.45, N 1.01. − For **3**, a different method of crystallisation was used. The filtered diethyl ether solution containing **3** was concentrated to dryness, the residue was dissolved in 10 mL of ethanol, followed by the dropwise addition of pentane until the solution became cloudy. Then the solution was cooled to −18 °C for a few days giving the $[N(PPh_3)_2]^+$ salt of **3** as dark-violet needles. The crystals were dried in vacuo. − **3**: Yield 76 mg (75%). − $C_{53}H_{40}IrNO_{11}P_2Ru_3 \bullet H_2O$ (1424.28): calcd. C 44.13, H 2.93, N 0.97; found C 43.96, H 2.76, N 1.02.

$[N(PPh_3)_2][Ru_2Ir(CO)_9(PhCCPh)]$ (Anion 6): A solution containing $[N(PPh_3)_2]$ $[Ru_3Ir(CO)_{11}(PhCCPh)]$ (anion **2**), prepared from 0.0715 mmol of **1** as described above, in Et_2O (20 mL) was placed in a pressure Schlenk tube and stirred at room temperature for 20 h under a pressure of 2 bar of CO. The colour changed from red-orange to wine-red, then to orange with precipitation of the $[N(PPh_3)_2]^+$ salt of **6** as a yellow powder. The precipitate was filtered off, washed with Et_2O (3 × 10 mL) and crystallised at room temperature by slow diffusion of Et_2O into a CH_2Cl_2 solution. The yellow crystals were dried in vacuo. **6**: Yield (with respect to **1**): 73 mg (75%). − $C_{59}H_{40}IrNO_9P_2Ru_2$ (1363.27): calcd. C 51.98, H 2.99, N 1.03; found C 51.68, H 2.99, N 1.04.

$[N(PPh_3)_2][Ru_2Ir(CO)_9(RCCR')]$ (Anions 7, 8, 9): A solution containing $[N(PPh_3)_2][Ru_3Ir(CO)_{11}(RCCR')]$ (**3**: R = R′ = Et; **4**: R = Ph; R′ = Me; **5**: R = R′ = Me), prepared from 0.0715 mmol of **1** as described above, in CH_2Cl_2 (25ml) was placed in a pressure Schlenk tube and stirred at 90 °C for 45 min under a pressure of 2 bar of CO. The colour changed, from red-orange to wine-red, then to orange. After removal of the solvent, the orange residue was washed with hexane (3 × 10 ml) to remove $Ru_3(CO)_{12}$ formed during the reaction. The remaining orange oil was dried and dissolved in 5−10 mL of ethanol, followed by the addition of pentane until the solution became cloudy. In the case of **8** no pentane was added. Then the solution was cooled to −18 °C for a few days which gave the $[N(PPh_3)_2]^+$ salt of **7** as yellow-orange crystals and the $[N(PPh_3)_2]^+$ salts of **8** and **9** precipitated as a yellow-brown powder. The solids were dried in vacuo. − **7**: Yield (with respect to **1**): 51 mg (56%). − $C_{51}H_{40}IrNO_9P_2Ru_2 \bullet 2.5\ H_2O$ (1267.19): calcd. C 46.65, H 3.42, N 1.06; found C 46.42, H 3.02, N 1.11. − **8**: Yield (with respect to **1**): 56 mg (60%). − $C_{54}H_{38}IrNO_9P_2Ru_2$ (1301.20): calcd. C 49.85, H 2.94, N 1.08; found C 49.66, H 3.16, N 1.16. − **9**: Yield (with respect to **1**): 49 mg (55%). − $C_{49}H_{36}IrNO_9P_2Ru_2$ (1239.13): calcd. C 47.50, H 2.93, N 1.13; found C 47.24, H 3.13, N 1.19.

$[HRu_2Ir(CO)_9(RCCR')]$ (10−13): To a solution of $[N(PPh_3)_2]$-$[Ru_2Ir(CO)_9(RCCR')]$ (anions **6**: R = R′ = Ph; **7**: R = R′ = Et; **8**: R = Ph; R′ = Me; **9**: R = R′ = Me) (0.0370 mmol) in CH_2Cl_2 (30 mL) a slight excess of $HBF_4 \bullet OEt_2$ (54%, 60 μL) was added under stirring. After 30 min, the solvent was evaporated, and the residue was dissolved in the minimum quantity of CH_2Cl_2. The solution was separated by thin-layer chromatography with a mixture of CH_2Cl_2 and hexane (1:6) as eluent. The yellow band containing the product was extracted with CH_2Cl_2, followed by concentration to dryness. The resulting yellow oil was dissolved in hexane and cooled to −18 °C to give yellow crystals of **10**−**13**. The crystals were dried in vacuo. − **10**: Yield 21 mg (68%). − $C_{23}H_{11}IrO_9Ru_2$ (825.69): calcd. C 33.46, H 1.34; found C 33.48, H 1.32. − **11**: Yield 18 mg (66%). − $C_{15}H_{11}IrO_9Ru_2$ (729.61): calcd. C 24.69, H 1.52; found C 24.51, H 1.54. − **12**: Yield 17 mg (60%). − $C_{18}H_9IrO_9Ru_2$ (763.62): calcd. C 28.31, H 1.19; found C 28.40, H 1.24. − **13**: Yield 16 mg (62%). − $C_{13}H_7IrO_9Ru_2$ (701.55): calcd. C 22.26, H 1.01; found C 22.12, H 1.04.

$[HRu_3Ir(CO)_{11}(RCCR')]$ (14−15): To a solution of $[N(PPh_3)_2]$-$[Ru_3Ir(CO)_{11}(RCCR')]$ (**2**: R = R′ = Ph; **3**: R = R′ = Et), prepared from 0.0715 mmol of $[N(PPh_3)_2]$**1** as described above, in 20 mL of Et_2O was added a slight excess of $HBF_4 \bullet OEt_2$ (54%,

Table 9. Crystallographic data and refinement details for compounds **2**, **4**, **5**, and **6**

	2	**4**	**5**	**6**
Formula	$C_{61}H_{40}O_{11}NP_2IrRu_3$ 0.25 C_6H_{14}	$C_{56}H_{38}O_{11}NP_2IrRu_3$	$C_{51}H_{36}O_{11}NP_2IrRu_3$	$C_{59}H_{40}O_9NP_2IrRu_3$
M	1520.42	1458.22	1396.16	1363.20
Crystal system	Triclinic	Triclinic	Triclinic	Triclinic
Space group	$P-1$	$P-1$	$P-1$	$P-1$
a [Å]	10.1350(8)	9.2769(10)	10.678(2)	10.5124(11)
b [Å]	15.5218(13)	16.7823(16)	15.741(4)	15.545(3)
c [Å]	19.8838(17)	17.2250(17)	15.705(3)	17.830(3)
α [°]	98.652(10)	88.034(12)	102.672(19)	100.04(2)
β [°]	99.163(10)	84.463(12)	91.363(12)	101.543(14)
γ [°]	94.583(10)	80.982(12)	103.730(13)	101.551(19)
V [Å^3]	3035.6(4)	2635.7(5)	2493.7(9)	2726.3(8)
Z	2	2	2	2
Crystal size [mm]	0.38 × 0.15 × 0.11	0.50 × 0.50 × 0.30	0.65 × 0.58 × 0.53	0.57 × 0.27 × 0.27
Colour	Dark-red	Black	Black	Yellow
D_c [g cm^{-3}]	1.687	1.837	1.859	1.661
μ [mm^{-1}]	3.028	3.482	3.675	3.097
Transmission factors: min/max	–	0.479/0.832	0.3979/0.6612	0.3427/0.3917
F(000)	1505	1416	1352	1336
θ limits [°]	2.13–25.88	2.38–25.88	2.10–25.48	2.01–25.49
hkl ranges	−12 to 11, −19 to 18, −24 to 24	−11 to 11, −20 to 20, −20 to 21	−12 to 12, −19 to 18, 0 to 19	−12 to 12, −18 to 18, 0 to 21
Reflections measured	23865	20460	9251	10126
Independent reflections	10950	9406	9251	10126
Observed reflections	7930	8994	8542	8153
$R1$ [$I > 2\sigma(I)$]/$R1$ (all data)[a]	0.0316/0.0483	0.0226/0.0240	0.0371/0.0433	0.0551/0.0778
$wR2$ [$I > 2\sigma(I)$]/$wR2$ (all data)[b]	0.0739/0.0783	0.0567/0.0576	0.1004/0.1107	0.1184/0.1334
Goodness of fit on F^2[c]	0.882	1.065	1.379	1.169
Maximum δ/σ	0.002	0.002	0.061	0.019
Largest diff. peak and hole [e Å^3]	1.070/−1.829	1.342/−1.125	1.580/−1.373	1.749/−1.457

[a] $R1 = \Sigma||F_o| - |F_c||/\Sigma|F_o|$. – [b] $wR2 = [\Sigma w(F_o^2 - F_c^2)^2/\Sigma w(F_o)^4]^{1/2}$. – [c] $S = [\Sigma w(F_o^2 - F_c^2)^2/(n - p)]^{1/2}$ (n: number of reflections; p: number of parameters).

Table 10. Crystallographic data and refinement details for compounds **10**, **12**, and **15**

	10	**12**	**15**
Formula	$C_{23}H_{11}O_9IrRu_2$	$C_{18}H_9O_9IrRu_2$	$C_{17}H_{11}O_{11}IrRu_3$
M	825.66	763.59	886.67
Crystal system	Triclinic	Triclinic	Triclinic
Space group	$P-1$	$P-1$	$P-1$
a [Å]	10.927(2)	9.1281(5)	8.0650(14)
b [Å]	14.480(3)	9.9456(6)	9.4766(13)
c [Å]	16.793(2)	12.6212(14)	16.423(4)
α [°]	70.080(13)	96.966(9)	96.392(19)
β [°]	85.071(17)	108.833(9)	101.47(2)
γ [°]	86.106(19)	96.349(7)	109.063(14)
V [Å^3]	2486.8(8)	1062.70(15)	1141.4(4)
Z	4	2	2
Crystal size [mm]	0.57 × 0.57 × 0.42	0.68 × 0.34 × 0.34	0.95 × 0.65 × 0.36
Colour	Yellow	Yellow	Red-orange
D_c [g cm^{-3}]	2.205	2.386	2.580
μ [mm^{-1}]	6.586	7.695	7.811
Transmission factors: min/max	0.0474/0.0845	0.0671/0.1236	0.0137/0.0460
F(000)	1544	708	820
θ limits [°]	2.20–25.47	2.09–25.48	2.32–25.46
hkl ranges	−13 to 13, −16 to 17, 0 to 20	−11 to 10, −12 to 11, 0 to 15	−9 to 9, −11 to 11, 0 to 19
Reflections measured	9223	3941	4324
Independent reflections	9223	3941	4234
Observed reflections	8141	3774	4134
$R1$ [$I > 2\sigma(I)$]/$R1$ (all data)[a]	0.0360/0.0441	0.0290/0.0309	0.0365/0.0387
$wR2$ [$I > 2\sigma(I)$]/$wR2$ (all data)[b]	0.0870/0.0920	0.0833/0.0849	0.1071/0.1127
Goodness of fit on F^2[c]	1.258	1.292	1.280
Maximum δ/σ	0.004	0.001	0.001
Largest diff. peak and hole [e Å^3]	0.916/−0.876	1.237/−0.987	1.831/−1.445

[a] $R1 = \Sigma||F_o| - |F_c||/\Sigma|F_o|$. – [b] $wR2 = [\Sigma w(F_o^2 - F_c^2)^2/\Sigma w(F_o)^4]^{1/2}$. – [c] $S = [\Sigma w(F_o^2 - F_c^2)^2/(n - p)]^{1/2}$ (n: number of reflections; p: number of parameters).

60 μL). After 30 min at room temperature, the white precipitate was filtered off, washed twice with 10 mL of Et_2O and then discarded. The solution was concentrated, the residue dissolved in CH_2Cl_2 (2 mL) and submitted to thin-layer chromatography (silica gel, CH_2Cl_2/hexane, 1:3). The product was extracted from the orange main band with CH_2Cl_2 and crystallised from hexane at

−18 °C. The orange air-stable crystals were dried in vacuo. − **14**: Yield (starting from **1**) 36 mg (51%). − **15**: Yield (starting from **1**) 29 mg (45%) − $C_{17}H_{11}IrO_{11}Ru_3$ (886.69): calcd. C 23.02, H 1.25; found C 23.21, H 1.30.

[$HRu_3Ir(CO)_{11}$(PhCCMe)] (16): A solution of [$HRu_3Ir(CO)_{13}$][9] (83 mg, 0.096 mmol) and PhC≡CMe (18 μL, 0.145 mmol) in hexane (30 mL) was stirred at 80−85 °C in a pressure Schlenk tube. During the reaction, the pressure was released once. After 1 h, the solution changed colour from red to orange. After removal of the solvent, the dark orange residue was dissolved in 5 ml of CH_2Cl_2 and submitted to thin-layer chromatography (silica gel, CH_2Cl_2/hexane, 1:3). From the orange main band, **16** was extracted with CH_2Cl_2 and crystallised from hexane at −18 °C. The orange air-stable crystals were dried in vacuo. − **16**: Yield 27 mg (31%) − $C_{20}H_9IrO_{11}Ru_3$ (920.71): calcd. C 26.09, H 0.99; found, C 26.02, H 0.99.

X-ray Structure Analyses: Single crystals of **2**, **4**, **5, 6**, **10**, **12**, and **15** were obtained as described under Preparations. Selected crystallographic data for the complexes are summarised in Tables 9 and 10, and selected bond lengths and bond angles are listed in Tables 2−8. Single-crystal X-ray diffraction data of the $[N(PPh_3)_2]^+$ salts of **2** and **4** were collected at room temperature and −50 °C, respectively with a Stoe Imaging Plate Diffractometer System (Stoe & Cie, 1995) equipped with a one-circle goniometer and a graphite monochromator. 200 exposures (3 min per exposure) were obtained at an image-plate distance of 70 mm with $0° < \phi < 200°$ and with the crystal oscillating through 1° in φ. The $[N(PPh_3)_2]^+$ salts of **5** and **6** and complexes **10**, **12**, and **15** were measured at room temperature with a Stoe-Siemens AED2 four-circle diffractometer using Mo-K_α graphite-monochromated radiation (λ = 0.71073 Å; ω-2θ scans). The structures of the $[N(PPh_3)_2]^+$ salts of **2**, **4**, **5**, **6**, and that of complex **15** were solved by direct methods, whereas those of **10** and **12** were solved by Patterson methods using the program SHELXS-97.[27] All the structures were refined by full-matrix least squares on F^2 with SHELXL-97.[28] The salt $[N(PPh_3)_2]$**2** crystallises with a quarter of a disordered molecule of hexane. The five carbon atoms C62A, C62B, C63A, C63B, and C64 were refined isotropically using the SHELXL-97 default parameters. In compounds $[N(PPh_3)_2]$**5** and $[N(PPh_3)_2]$**6** one of the carbonyl ligands is found to be disordered and has been split into C6A-O6A and C6B-O6B (anion **5**), C21A-O21A and C21B-O21B (anion **6**), respectively, with an occupancy of a half for each atom. The position of the hydride ligands in **10**, **12**, and **15** were located from Fourier difference maps and refined isotropically, while the remaining hydrogen atoms of the methyl, ethyl or phenyl substituents were included in calculated positions and treated as riding atoms with SHELXL-97 default parameters. For $[N(PPh_3)_2]$**4**, an empirical absorption correction was applied using DIFABS[29] and for $[N(PPh_3)_2]$**5**, $[N(PPh_3)_2]$**6**, **10** **12**, **15** it was based on ψ scans.[30] The Figures were drawn with ORTEP[31] (thermal ellipsoids, 50% probability level). Complete tables of bond lengths and angles and lists of thermal parameters have been deposited with the Cambridge Crystallographic Data Centre, 12 Union Road, Cambridge CB2 1EZ, UK. Copies of the data can be obtained free of charge on application to CCDC, 12 Union Road, Cambridge CB2 1EZ, UK [Fax: int. code + 44-1223/336-033; E-mail: deposit@ccdc.cam.ac.uk], on quoting the deposition numbers CCDC-111752−111758.

Acknowledgments

We thank the Fonds National Suisse de la Recherche Scientifique for financial support of this work. A generous loan of ruthenium(III) chloride hydrate from the Johnson Matthey Research Centre is gratefully acknowledged.

[1] R. D. Adams, in *Comprehensive Organometallic Chemistry 2* (Eds.: E. W. Abel, F. G. A. Stone, G. Wilkinson), Elsevier, Oxford, **1995**, vol. 10, p. 1.
[2] Y. Chi, D. K. Hwang, in *Comprehensive Organometallic Chemistry 2* (Eds.: E. W. Abel, F. G. A. Stone, G. Wilkinson), Elsevier, Oxford, **1995**, vol. 10, p. 85.
[3] [3a] P. Braunstein, J. Rosé, in *Comprehensive Organometallic Chemistry 2* (Eds.: E. W. Abel, F. G. A. Stone, G. Wilkinson), Elsevier, Oxford, **1995**, vol. 10, p. 351. − [3b] For a general review see: *Catalysis by Di- and Polynuclear Metal Cluster Complexes* (Eds.: R. D. Adams, F. A. Cotton), Wiley-VCH, Chichester, **1998**. − [3c] R. D. Adams, T. S. Barnard, Z. Li, W. Wu, J. H. Yamamoto, *J. Am. Chem. Soc.* **1994**, 116, 9103. − [3d] R. D. Adams, T. S. Barnard, *Organometallics* **1998**, 17, 2567. − [3e] R. D. Adams, T. S. Barnard, *Organometallics* **1998**, *17*, 2885.
[4] E. Sappa, A. Tiripicchio, A. J. Carty, G. E. Toogood, *Prog. Inorg. Chem.* **1987**, *35*, 437 and references therein.
[5] P. R. Raithby, M. J. Rosales, *Adv. Inorg. Chem. Radiochem.* **1985**, *29*, 169.
[6] E. L. Muetterties, T. N. Rhodin, E. Band, C. F. Brucker, W. R. Pretzer, *Chem. Rev.* **1979**, *79*, 91.
[7] A. Fusi, R. Ugo, R. Psaro, P. Braunstein, J. Dehand, *J. Mol. Catal.* **1982**, *16*, 217.
[8] V. Ferrand, G. Süss-Fink, A. Neels, H. Stoeckli-Evans, *J. Chem. Soc., Dalton Trans.* **1998**, 3825.
[9] G. Süss-Fink, S. Haak, V. Ferrand, A. Neels, H. Stoeckli-Evans, *J. Chem. Soc., Dalton Trans.* **1997**, 3861.
[10] O. Benali-Baitich, J. C. Daran, Y. Jeannin, *J. Organomet. Chem.* **1988**, *344*, 393.
[11] M. Cazanoue, N. Lugan, J. J. Bonnet, R. Mathieu, *Organometallics* **1988**, *7*, 2480.
[12] [12a] P. Braunstein, J. Rosé, *J. Organomet. Chem.* **1983**, *252*, C101. − [12b] E. Roland, H. Vahrenkamp, *Organometallics* **1983**, *2*, 1048.
[13] D. E. Fjare, W. L. Gladfelter, *J. Am. Chem. Soc.* **1984**, *106*, 4799.
[14] R. H. Crabtree, M. Lavin, *Inorg. Chem.* **1986**, *25*, 805.
[15] K. Wade, *Adv. Inorg. Chem. Radiochem.* **1976**, *18*, 1.
[16] J. C. Wang, Y. Chi, S.-M. Peng, G.-H. Lee, S.-G. Shyu, F.-H. Tu, *J. Organomet. Chem.* **1994**, *481*, 143.
[17] M. Bergamo, T. Beringhelli, G. Dalfonso, P. Mercandelli, M. Moret, A. Sironi, *Organometallics* **1997**, *19*, 4129.
[18] S. Deabate, R. Gordiano, E. Sappa, *J. Cluster Sci.* **1997**, *8*, 407.
[19] E. Roland, W. Bernhardt, H. Vahrenkamp, *Chem. Ber.* **1985**, *118*, 2858.
[20] S. Aime, R. Gobetto, L. Milone, D. Osella, L. Violano, A. J. Arce, Y. De Sanctis, *Organometallics* **1991**, *10*, 2854.
[21] D. Boccardo, M. Botta, R. Gobetto, D. Osella, A. Tiripicchio, M. Tiripicchio-Camellini, *J. Chem. Soc., Dalton Trans.* **1988**, 1249.
[22] [22a] J. Evans, G. Mc Nulty, *J. Chem. Soc., Dalton Trans.* **1981**, 2017. − [22b] D. Boccardo, M. Botta, R. Gobetto, D. Osella, A. Tiripicchio, M. Tiripicchio-Camellini, *J. Chem. Soc., Dalton Trans.* **1988**, 1249. − [22c] M. A. Gallop, B. F. G. Johnson, R. Khattar, J. Lewis, P. Raithby, *J. Organomet. Chem.* **1990**, *386*, 121.
[23] [23a] F. W. B. Einstein, K. G Tyers, A. S. Tracey, D. Sutton, *Inorg. Chem.* **1986**, *25*, 1631. − [23b] A. J. Deemings, *J. Organomet. Chem.* **1978**, *150*, 123.
[24] J. T. Park, J. R. Shapley, M. Rowen Churchill, C. Bueno, *J. Am. Chem. Soc.* **1983**, *105*, 6182.
[25] J. T. Park, J. R. Shapley, C. Bueno, J. W. Ziller, M. Rowen Churchill, *Organometallics* **1988**, *7*, 2307.
[26] D. D. Perrin, W. L. F. Armarego, *Purification of Laboratory Chemicals*, 3rd ed., Pergamon Press, Oxford, **1988**.
[27] G. M. Sheldrick, *Acta Crystallogr., Sect. A* **1990**, 46, 467.
[28] G. M. Sheldrick, *SHELXL-97, Program for crystal structure refinement*, University of Göttingen, Germany, **1997**.
[29] N. Walker, D. Stuart, *Acta Crystallogr., Sect. A* **1990**, *46*, 158.
[30] A. C. T. North, D. C. Phillips, F. C. Mathews, *Acta Crystallogr., Sect. A* **1968**, *24*, 351.
[31] C. K. Johnson, *ORTEP*, Oak Ridge National Laboratory, Oak Ridge, TN, modified for PC by L. Zsolnai, H. Pritzkow, University of Heidelberg, Germany, **1994**.

Received November 30, 1998
[I98407]